HIGH SCHOOL EDITION
Journal of Student Research
Volume 13 Issue 3 (2024)

Corrugated Airfoil Shape Effect on Aerodynamic Efficiency of a 3D Printed Remote Control Plane

Gracye Lamb[1] and John Murnan[#]

[1]Etowah High School, USA
[#]Advisor

ABSTRACT

Early wind tunnel experiments and subsequent studies have shown that corrugated wings offer comparable or superior aerodynamic efficiency to smooth wings, with computational fluid dynamics (CFD) confirming these benefits. However, the effects of turbulence on these designs and their practical application to Micro Air Vehicles (MAVs) has yet to be thoroughly tested. A two-part experimental method involving CFD analysis and flight time tests was employed to evaluate the impact of various corrugated wing designs on the performance of an MAV, with a smooth airfoil as a control, aiming to measure aerodynamic efficiency through lift-to-drag ratios and flight times. The experiment found that that there was no significant correlation between lift-to-drag ratios and total flight times, though a minor positive correlation existed between flight times and speed and minor negative correlation with flight times and mass, and a moderately strong inverse correlation was found between speed and mass. The study found that corrugated airfoils generally can improve aerodynamic efficiency, though results varied significantly, indicating that not all corrugated designs are equally beneficial. Further, while CFD analysis showed inconsistencies compared to previous studies, it highlighted that the turbulent atmospheric layer impacts real-world aerodynamic performance, suggesting that CFD alone may not reliably predict flight efficiency of corrugated wings.

Introduction

Biomimetics attempts to take the physiological attributes of evolved organisms and utilize them in engineering solutions (Rose et al., 2021). Since every species abides by the rules of natural selection as discovered by Charles Darwin, hereditary traits have been optimally evolved according to their surrounding environment for billions of years. By not considering the evolutionary design process in current designs, engineering innovations would be delayed. Therefore, bioinspired innovations in aerospace engineering have been developed for over 3000 years (Rose et al., 2021). Biomimetic solutions offer higher efficiency and adaptability than traditional designs, with inspiration coming from plants, birds, aquatic animals, and even insects. For example, bristles surrounding a dandelion seed generate a low-pressure vortex bubble above the dandelion, creating suction and enhancing lift for seed dispersal (Rose et al., 2021). The leading edge (LE) serrations, or upward bending barb tips of a barn owl wing, reduce noise and demonstrate improved aerodynamic efficiency (Rose et al., 2021). The rough placoid scales of a mako shark covered in grooves contribute to the drag reduction of sharks (Rose et al., 2021). For this paper, the focus will be on corrugated, or wavy, wings of insects (see Figure 1) and their effect on aerodynamic efficiency when applied to aeronautical designs.

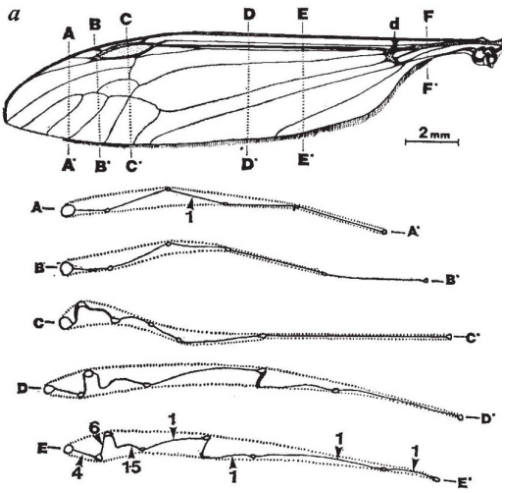

Figure 1. Corrugated insect wing cross sections that are not smooth, but instead have folds (Rees, 1975b).

Literature Review

First Experiments

An early wind tunnel test conducted by Rees (1975a) formed the foundation of research on corrugated wings by comparing the lift and drag coefficients, or the ratio of the lift/drag force to the dynamic pressure force times the area of the wing (Kurak, 2022a; Kurak, 2022b), of a hoverfly wing section and its smooth counterpart (see Figure 2). The tests were completed at lower Reynolds numbers (Re) of 450, 800, and 900. These numbers label the flow regime, where lower numbers describe sheet-like and calm laminar flow ($Re<5x10^5$) and higher numbers describe chaotic and turbulent flow ($Re>5x10^5$) (Rose et al., 2021). The polar plots, or graphs that convey the relationship between lift and drag, revealed that the corrugated wing had similar characteristics to the smoothed envelope wing. Additionally, Figure 3 presents the fluid flow around the corrugated wing, displaying how the fluid became trapped in the folds of the corrugations and then slowly rotated, causing the main flow to avoid these areas and behave as if it were more of an enveloped profile (Rees, 1975a). Another study performed by Rees (1975b) assessed the load-bearing characteristics, specifically deflection and maximum stress, of a corrugated and flat beam. It was found that with the introduction of corrugations, there is barely an increase in weight while also reducing the deflection and maximum stress of a given load (Rees, 1975b). Therefore, Rees's studies communicate that corrugated wings have all the advantages of low mass and high stiffness while also demonstrating no obvious aerodynamic shortcomings compared to a smoothed wing.

Figure 2. Top: corrugated wing cross section of a hoverfly. Bottom: smooth counterpart cross section made by drawing an "envelope" around the corners of the corrugations (Rees, 1975a).

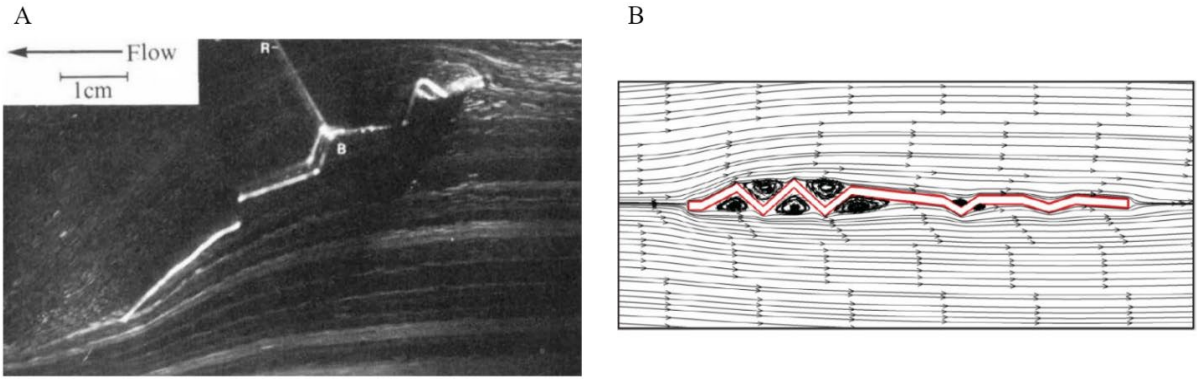

Figure 3. Figure 3A depicts fluid flow from Rees's (1975a) experiment that was made visible by electrolytically releasing hydrogen bubbles from a wire upstream. The region labeled "B" is one of the folds where fluid becomes trapped and starts to circulate. Figure 3B illustrates computer-generated streamlines of the flow around a corrugated wing (Abd El-Latief et al., 2019). The main flow ignores the corrugations and goes around the fluid that circulates in the valleys.

While Rees's findings demonstrated similar aerodynamic performance, Okamoto et al. (1996) found there is increased performance with surface waviness. Model wings went under a wind tunnel test to analyze a variety of shape characteristics, indicating that thinner, positive cambered (upwardly convex), and wavy profiles achieved higher lift production and a maintained drag value. However, not all waviness shapes were equal as the model with a downward facing LE (see Figure 4) performed better than the upward facing model (Okamoto et al., 1996). A turbulence assessment, constructed by placing a lattice of aluminum cylinders into the wind tunnel, expressed a higher lift and lower drag in turbulent flow of the wavy model compared to the measurements in laminar flow, suggesting better performance (Okamoto et al., 1996). Two dragonfly wings were then examined for aerodynamic characteristics using the wind tunnel, giving comparable results to the positive camber model (Okamoto et al., 1996). As insect wings are not smooth surfaces, the study portrays corrugated surfaces as favorable in terms of aerodynamic characteristics.

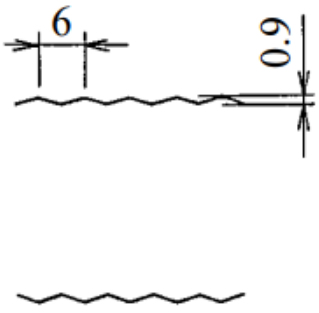

Figure 4. LE, or front edge of the wing, contributes to the performance of the wing. When the flow is moving from left to right, the top wing is an example of a downward facing LE and the bottom wing is an example of an upward facing LE (Okamoto et al., 1996).

Luo and Sun (2005) compared the aerodynamic forces and flow distribution between a corrugated wing based upon a fruit fly and a flat plate with the same planform, or top view of a wing, and thickness. The lift and drag coefficients were found to be almost identical for both wings, agreeing with the results of Rees

(1975a). The surface pressure distributions suggested that the lift value of the corrugated wing was not higher than the flat plate as the folds only produced a local change in pressure, so these differences could not increase the total lift force. Furthermore, since the main flow of a corrugated wing acts as if there are no folds, they argued that the wing would have to possess about the same force measurements as its smooth counterpart (Luo & Sun, 2005). While the outcomes of these early studies differed in the lift production of the corrugated profiles, all agree that there are no aerodynamic deficiencies with wavy designs.

CFD Experiments

Newer computational fluid dynamics (CFD) experiments agree with Okamoto et al. (1996) with the fact their computer-generated results exhibit superiority of corrugated airfoils. Jain et al. (2015) investigated the change in aerodynamic performance of a Mueller C4 (smooth) airfoil when corrugations were applied, ranging from one to five corrugations stretching to mid-chord length, or middle of the profile, at an angle of attack of 5 degrees and Re=10,000. All the modified airfoils presented a higher lift and drag than the original airfoil, with the least number of corrugations producing the most drag. The airfoils containing two to five corrugations experienced higher aerodynamic efficiency (lift to drag ratio), where the model with four corrugations had a ratio of 17.94, a 21% increase from the baseline model's ratio of 15.76 (Jain et al., 2015). Furthermore, the pressure distribution streamlines for the corrugated models revealed that the recirculation regions in the valleys lead to higher suction on the top surface (suction side) of the airfoils and increased pressure on the bottom surface (pressure side), resulting in a larger pressure difference between surfaces (Jain et al., 2015). This phenomenon caused the increased production in lift, therefore giving the corrugated and wavy profiles better performance in the two studies.

Similarly, Abd El-Latief et al. (2019) based their study on the mid-wing cross section of a dragonfly, its smooth equivalent, and a flat plate at Re=200 and 1400, determining that the corrugated wing possessed a higher lift coefficient and lift to drag ratio, along with a comparable and sometimes lower drag coefficient to the smooth wing at all angles of attack, even when the recirculating flow regions escaped the valleys at greater angles. While the higher production of lift coincides with the other CFD study, the drag results contrast with all the previous studies as they always had a higher or similar drag value compared to the smooth profile. The flat plate generated almost the same coefficients as the corrugated wing, and even acquired superior performance at 5 and 10 degrees at Re=1400 (Abd El-Latief et al., 2019). Therefore, the structural performance of the corrugated wing and flat plate at various thicknesses were juxtaposed by applying uniform pressure on one side of the airfoils to measure stiffness. The flat plate that corresponded to the thickest portion of the corrugated wing deformed almost 60mm more than the wavy design and was not comparable until the thickness of the flat plate contributed to the weight being four times larger than that of the corrugated airfoil (Abd El-Latief et al., 2019), corroborating Rees's (1975b) study in that corrugated wings are characterized by high stiffness. The CFD experiments portray corrugated profiles as the preferable choice in terms of both aerodynamic efficiency and high stiffness at a minimal weight.

Differences in Corrugation Designs

Just as the study by Jain et al. (2015) compared different corrugated shapes, Kesel (2000) examined three cross sections of a dragonfly and their corresponding "filled" profiles to discover if there were dramatic differences in aerodynamic characteristics at Re=10,000 (see Figure 5). Dragonflies were used as the subject because they are one of the few successful insect gliders, who can glide up to 30 seconds without any noticeable loss in altitude (Abd El-Latief et al., 2019). Cross section 3 obtained the greatest gliding ratio, or aerodynamic efficiency, of 7.868, followed by profile 1 (7.351) and 2 (6.528). Each was greater than the filled profile values, continuing the pattern formed by the CFD studies. The overall quantities of profile 1 and 3 were very close

together, suggesting that LE orientation does not dramatically affect aerodynamic characteristics as their LEs were in opposite directions. This is an opposing opinion to Okamoto et al. (1996), who declared that aerodynamic characteristics shifted depending on LE orientation. Reducing the Reynolds number from 10,000 to 7,800 led to a drop in profile 1's gliding ratio by 16.6% (Kesel, 2000), backing up Okamoto et al. (1996) in that corrugated airfoils perform better in turbulent flow.

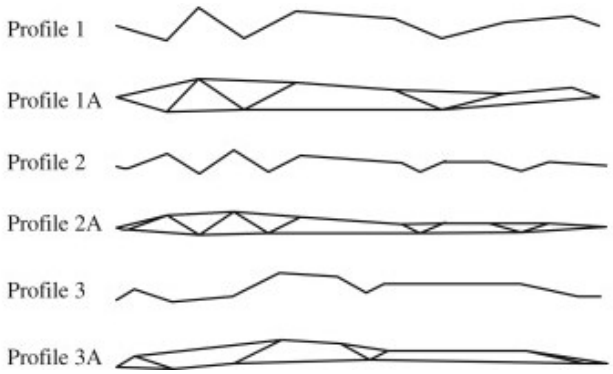

Figure 5. Profiles 1, 2, and 3 in Kesel's (2000) experiment were cross sections taken from a dragonfly wing. Their corresponding filled profiles were named profile 1A, 2A, and 3A (Kim et al., 2009).

Likewise, Kim et al. (2009) took cross section 1 from Kesel's (2000) study and compared them to five modified versions (see Figure 6) at Re=1400 to explore the influence of suction vs pressure side corrugations at Re=150. Modified model 1 contained only the corrugations of profile 1 on the suction side and demonstrated no change in lift from profile 1A, while modified model 2 contained the corrugations on the pressure side and exhibited similar lift to profile 1 (Kim et al., 2009). These findings suggest that corrugations on the suction side of an airfoil do not contribute substantially to lift production, but rather pressure side corrugations do. Modified model 3 was characterized by uniform pressure side corrugations from the leading to the trailing edge, with modified model 4 possessing shallower folds. They each generated a lift coefficient less than that of profile 1 and modified model 2 (Kim et al., 2009), indicating that a wide corrugation central on the pressure side is key to increasing lift. Modified model 5 exclusively incorporated pressure side corrugations near the LE and only produced a greater lift than profile 1A and modified model 1 (Kim et al., 2009). Therefore, its corrugated design is practically ineffective and offers an explanation as to why Luo & Sun (2005) did not see an increase in lift since their model only included LE corrugations. Depending on the design shape of a corrugated airfoil, the lift production can vary and may be the same as its filled in counterpart.

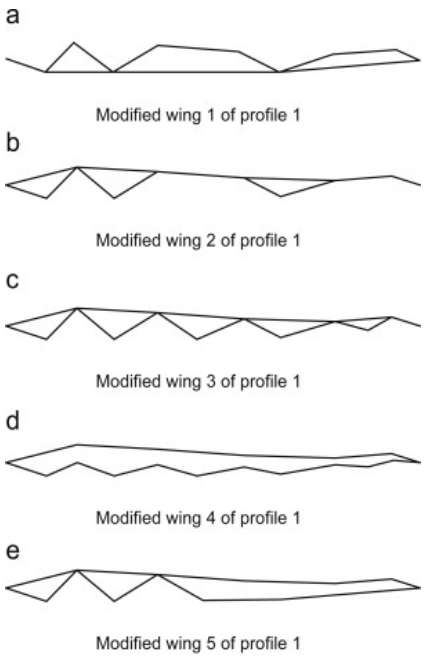

Figure 6. Profiles of the modified models in the experiment conducted by Kim et al. (2009).

Effect of Higher Turbulence/Research Gap

Since the aeronautical applications of corrugated wings would most likely be used in the turbulent atmospheric layer, where the wake of buildings and other structures generate turbulence, Biradar et al. (2022) addresses the effect of free stream turbulence on these airfoils at ultra-low Reynolds numbers (Re=960-11,700). In a water tunnel experiment with a fixed turbulence intensity of 6%, the shear layer that forms the smooth airfoil around the corrugations was observed to break down and collapse (Biradar et al., 2022). At higher Reynolds numbers, the thickness of the shear layer reduced so much that the streamlines converged toward the surface of the corrugated airfoil and stopped the flow from recirculating in the valleys. This change in strength is due to the interaction of turbulent flow with the peaks of the corrugated structures, which forces the main flow to mix with the low-pressure vortex regions of the valleys (Biradar et al, 2022). Therefore, turbulence results in flow moving closer to the surface and reduced aerodynamic efficiency, contrasting with the findings of Okamoto et al. (1996) who found that higher turbulence equated with better performance. Either way, corrugated airfoils are sensitive to turbulence intensity and should be considered when applying to aircraft.

The studies within the body of literature agree that corrugated wings would be a potential benefit when applied to Micro Air Vehicles (MAVs), or remotely controlled aircraft, because they fly within the low Reynolds number range where insect flight dominates. The design's low weight while simultaneously producing equal or greater lift than a smooth airfoil in theory would increase aerodynamic efficiency. However, none of the studies applied their findings to an actual MAV design to test the effect of corrugated airfoils in a real-life situation. Therefore, the present study will address the gap between tests on the wings themselves to the effect of attaching these wings to an MAV by comparing two values of aerodynamic efficiency—computer generated lift to drag ratio and flight time of a physical air vehicle. It will also act as another perspective on the effect of turbulence on corrugated airfoils as it will observe how the turbulent atmospheric layer changes the lift production outside of a closed system. Thus, the focus will be on the question: How do different types of corrugated airfoil shapes affect the aerodynamic efficiency of a 3D printed remote control plane?

Methods

A two-part experimental method was used in order to answer the research question, first a CFD analysis and then a flight time test. This method most effectively discovers the outcome of corrugations on plane wings, with the independent variable, or different corrugated designs, affecting the dependent variable, or varying performance of an MAV. Furthermore, only an experimental method was used in the studies in the body of literature, so it would only be natural to continue this pattern. A smooth airfoil was included in the study, serving as the control variable to base the change in values off of. By finding two forms of aerodynamic efficiency—lift to drag ratio and time of flight—quantitative data could be assessed and compared within Excel to determine the quality of corrugated airfoils on MAV designs compared to that of a smooth airfoil.

CFD Analysis

A computational fluid dynamics analysis of profile 1 and 1A (see Figure 5) from Kesel's (2000) study and the modified models of profile 1 (see Figure 6) from Kim et al.'s (2009) study was completed. The profiles were first created within Autodesk Inventor (see Figure 7/8), a 3D computer modeling program, and then transferred into Autodesk CFD, a finite element analysis program, where the lift and drag force of the airfoils could be calculated. From here, these force values were plugged into the lift and drag coefficient equations (see Equations 1 and 2). The air density was set to 1.225 kg/m^3, the standard density of air at 15°C and sea level (Helmenstine, 2020), and the velocity of each wing was set to the corresponding velocity found in experiment two for each wing. The lift to drag ratio, a measurement of aerodynamic efficiency, of each airfoil was then found by dividing their respected lift coefficient by their drag coefficient.

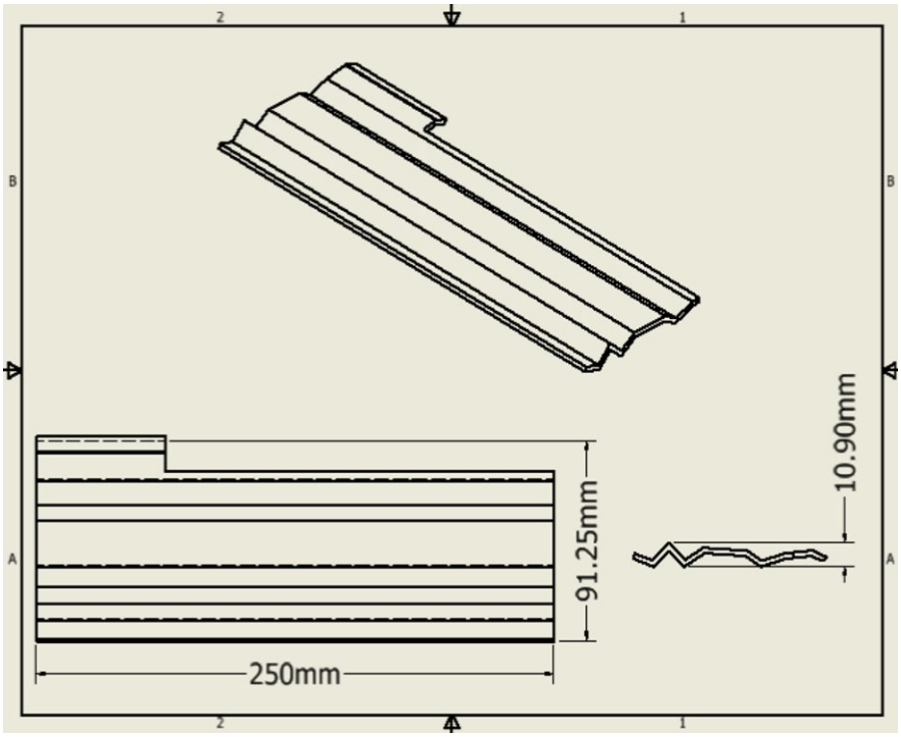

Figure 7. Profile 1 Autodesk Inventor Drawing with Dimensions. The dimensions noted for the height, width, and span of the wing in millimeters were followed for each of the other experimental wings in order to minimize variables. The thickness of the wings was set to 2.5mm.

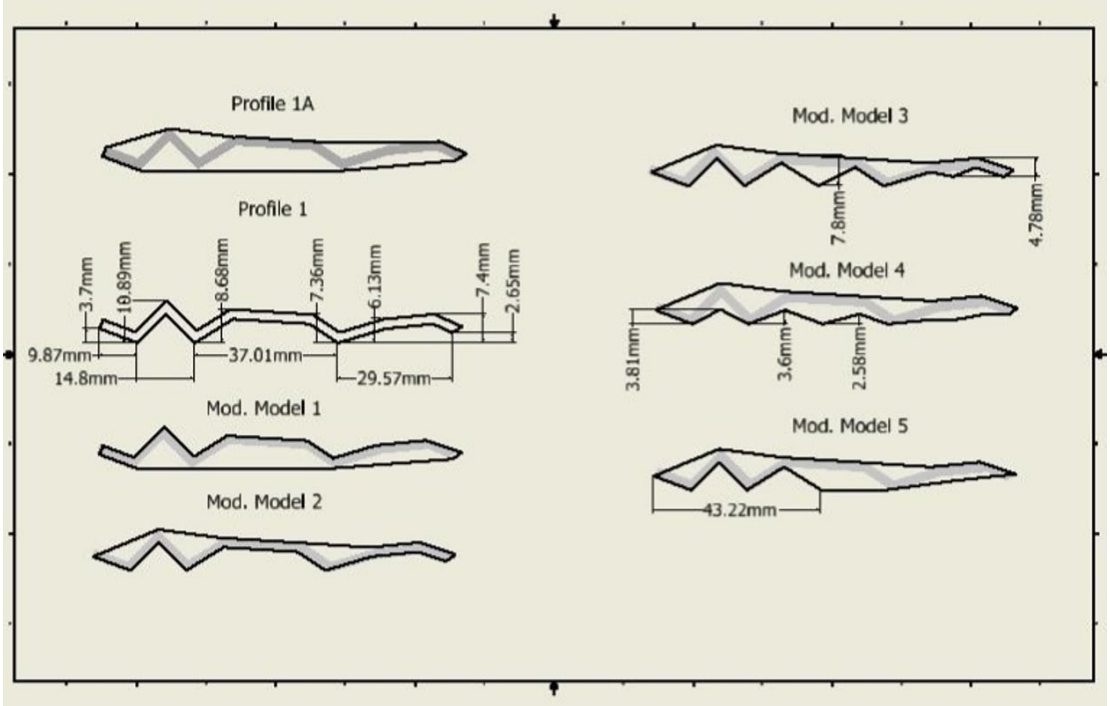

Figure 8. Dimensions of Each Profile Cross Section in Autodesk Inventor. The black lines outline the plane cross sections, with the light grey demonstrating how each profile was created from profile 1.

Equation 1: Below is the coefficient of lift (C_L) equation (Benson, 2021). L is the lift force, ρ is the air density, A is the surface wing area, and V is the velocity of the wing.

$$C_L = \frac{2L}{\rho A V^2}$$

Equation 2: Below is the coefficient of drag (C_D) equation (Hall, 2022). D is the drag force, ρ is the air density, A is the surface wing area, and V is the velocity of the wing.

$$C_D = \frac{2D}{\rho A V^2}$$

MAV Assessment

A single plane body (see Figure 9/10) was constructed within Autodesk Inventor in such a way that each of the wing profiles could be attached to the same plane body (see Figure 11) to control extraneous variables in the flight time experiment. The body and airfoils were then 3D printed with PETG filament due to its resistance to high temperatures, minimal susceptibility to warping, and being ideal for objects that experience sudden or sustained stress (All3DP, 2022). With a high risk of electrical components overheating and the plane crashing, along with the desire to avoid any inconsistencies between the computer generated profiles and 3D printed profiles, PETG filament was the leading choice. The mass of each wing pair was measured in grams using a digital scale. Figure 12 illustrates how the 3D printed parts were assembled with electrical equipment to create a remote control plane.

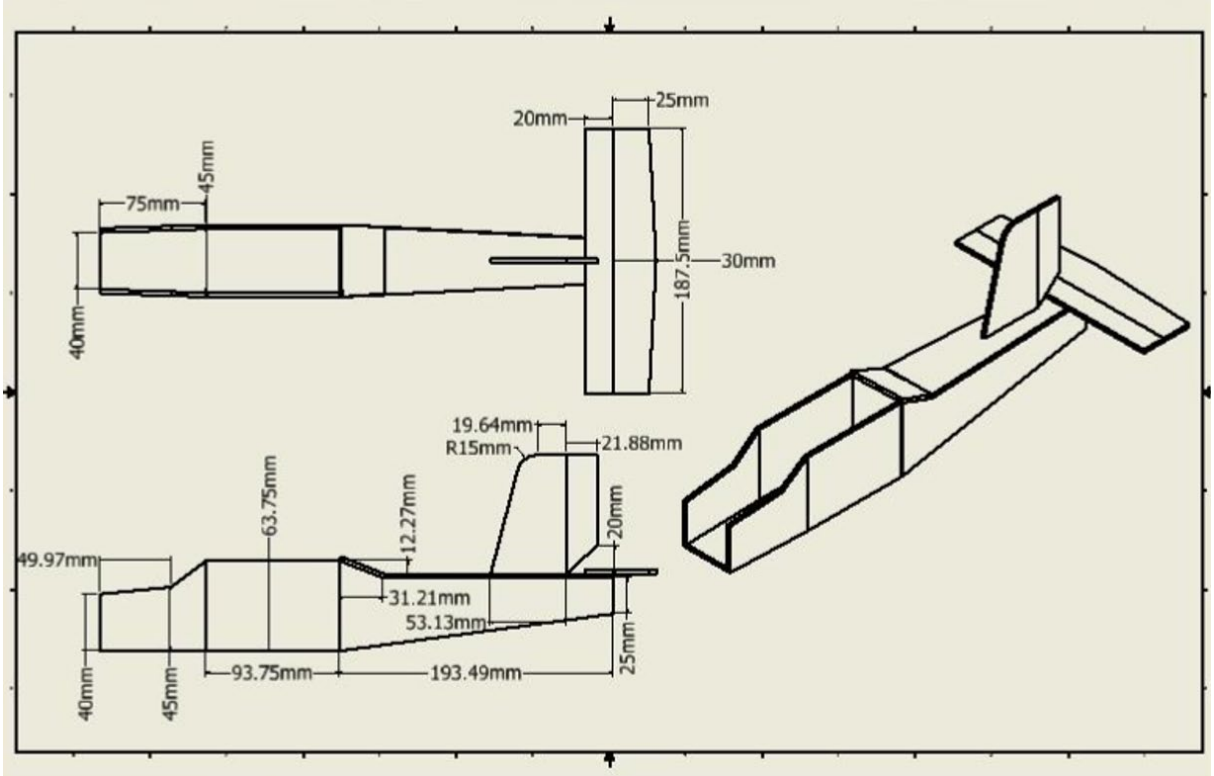

Figure 9. Dimensions of Plane Body in Autodesk Inventor. The frame/body of the plane was developed using KendinYap's (2020) design in Inventor and then 3D printed. The airfoil designs were also 3D printed from Inventor.

Figure 10. Above is the assembled 3D printed remote control plane that was used for each flight time and speed trial. All individual parts were 3D printed, except for the 4x4cm, 5/8 inch thick, piece of plywood at the front of the plane, and superglued/taped together. The motor was mounted to this piece of wood with 3/4 inch screws. Two 4x3 inch pieces of wood were superglued on either side of the frame underneath the wings for extra support.

A

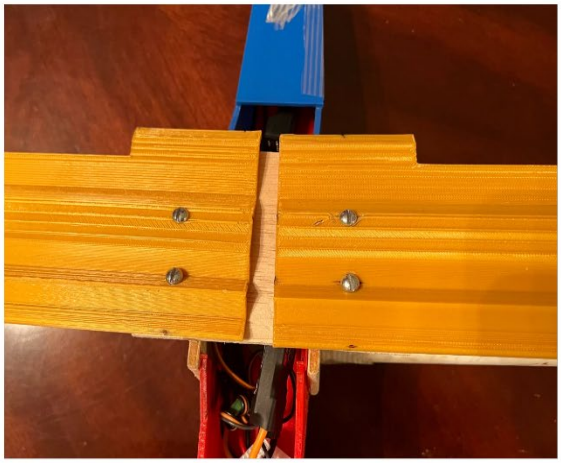

B

Figure 11. Above is the design that allowed each wing pair to be attached and detached from the plane body. A 7x3 1/2 inch piece of wood was glued to the top of the frame, and the wings were mounted and held in place with four 3/4 inch flathead bolts and nuts.

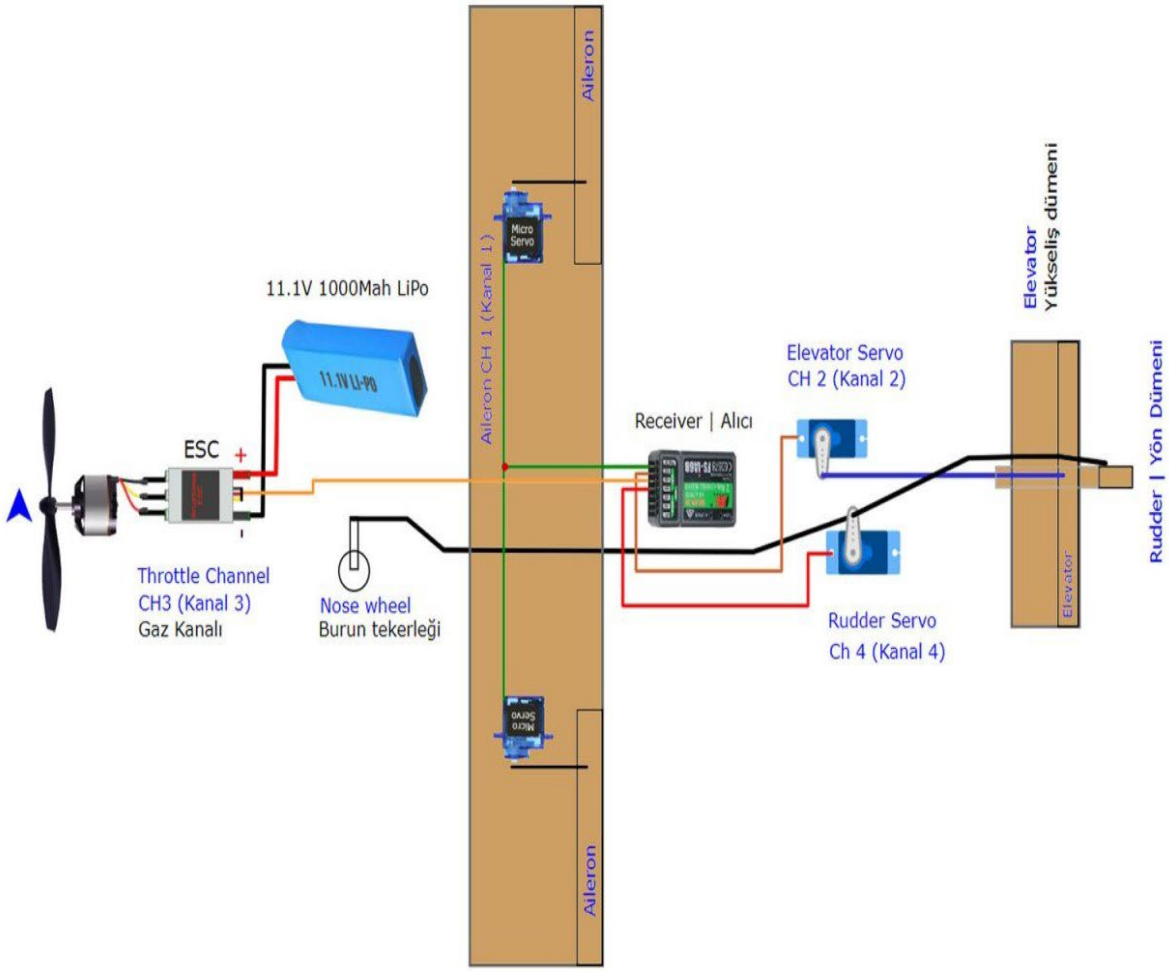

Figure 12. Diagram of Electronic Parts to Create Thrust for Remote Control Plane. Battery-1300mAh 45C 3S 11.1V Lipo, Motor-2200KV Brushless Outrunner, Transmitter/Receiver-Flysky FS-i6X 6-10 Channel, ESC-40A, Charger-Havcybin Lipo battery balance charger 80W, Propeller-3.17mm shaft diameter, Servos-9g (not used in final experiment), Wheel-40mm diameter foam (not used in final experiment). All parts fit inside the frame of the plane (KendinYap, 2020).

Due to the researcher's limited knowledge of electronic parts and inexperience with flying remote control planes, the plane was not actually able to take off and stay above ground for an extended period, making it impossible to gather total flight time data. The method was modified to keep the plane in the turbulent atmospheric layer and remove the user error involved with using a transmitter. Figure 13 shows the experiment's configuration created by a 2 ft orange PVC pipe with a diameter of 1 1/4 inches set in a 5-gallon bucket and held in place with cement. Another 2 ft white PVC pipe with a tee joiner attached to the top was placed inside the orange PVC, this time with a diameter of 1 inch. Five more white PVC pipes were attached to either side of the tee joint, three on one side and two on the other, with 2-inch coupling joiners attaching one horizontal PVC pipe to the next. The third PVC pipe measured to be 17 inches and held the plane in place with a 1 1/2-inch flathead bolt and nut. The circular path of the setup measured to have a radius of 1.65 meters and circumference of 10.37 meters.

Figure 13. MAV Experiment Setup in Turbulent Atmospheric Layer. Above is the setup for the flight time/speed experiments made of PVC pipes. A log was placed on the 5-gallon bucket to stabilize the system during flight trials.

Three trials for each wing pair were completed by allowing the plane to fly until battery failure, tracking the duration of the flight of each trial in seconds, and then the times were averaged. Three speed trials were also conducted by tracking the time in seconds it took the plane to complete 25 revolutions, averaging the three values together. From here, the total distance that the plane flew in 25 revolutions, which was found to be 259.25 meters, was divided by the average time to calculate the average speed in m/s.

Comparison of Data

The values from the present experiments were compared to determine if corrugated airfoils and their different designs affected the aerodynamic efficiency of an MAV. To discover if computer generated results are reliable and to observe the effect of the turbulent atmospheric layer on MAVs, the CFD lift to drag ratio results and flight times of each profile were compared. This was accomplished by calculating the correlation coefficient, or the measurement of the strength of the relationship between the two variables, within Excel. Positive values indicate a positive correlation and negative values indicate a negative correlation, with a scale of –1 to 1. A scatter plot with a line of best fit was also composed to visually communicate a potential pattern between the simulated and real-life aerodynamic efficiency of the profiles. A correlation coefficient and scatter plot were also created for the relationship between the other variables (flight time vs speed, flight time vs mass, speed vs mass).

Results

After completing the experiment, it was found that the lift to drag ratios of the profiles ranged from 0.010 to 0.321, making the largest value approximately 33 times more than the smallest value. Mod. Model 2 generated the lowest lift to drag ratio, and Mod. Model 1 generated the highest. Since the CFD analysis was the first portion of the study, it was expected that the wide range trend would continue when testing the other variables, specifically total flight time and speed. However, while the lift to drag ratios varied greatly, the average total flight times were more consistent between airfoils, spanning a time of 615 to 677 seconds before battery failure, or 10 minutes, 15 seconds to 11 minutes, 17 seconds. Profile 1 ran for the shortest amount of time, while Mod. Model 4 ran for the longest. Similarly, the speed of each pair of wings fell between 6.38 and 6.90 meters per

second, an 8.15 percent increase from the slowest to the fastest speed. The application of the Mod. Model 3 wings led to the slowest of all the flights, and Mod. Model 4 led to the fastest of all the flights. Interestingly, Mod. Model 4 was both the fastest pair of wings and demonstrated the longest flight time, indicating it was the most efficient of the profiles in the MAV assessment, but Mod. Model 3 came in second for total flight time with an average of 664 seconds while being the slowest of all the airfoils. The mass of each pair of wings was relatively close together, this being due to each airfoil having been created from profile 1. They ranged from 128 grams, set by Mod. Model 2 and Mod. Model 4, to 145 grams, set by profile 1A. Mod. Model 4 having the least mass of the wing pairs could offer an explanation for its ability to be the most efficient of the wings. Table 1 communicates the measurements taken of each profile during the study.

When comparing the lift to drag ratios and their corresponding total flight times, no significant pattern could be found, contrary to the belief that there would be a direct relationship between the two variables (see Figure 14). With a correlation coefficient of 0.02, the results were insignificant and could not be used to predict the total flight time from the lift to drag ratio or vice versa. As the two variables are measurements of aerodynamic efficiency, they would be related to one another in a perfect world/experiment. A possibility for this not occurring is that there were sources of error during data collection (i.e., degradation of the battery, differing temperatures during trials, varying wind speeds) that made some characteristics of the experiment vary from trial to trial or over the days that the experiment took place. Another potential explanation is that the relative roughness of the air within the turbulent atmospheric layer significantly affects the aerodynamic efficiency of a wing, although there is no evidence whether the turbulence improves or diminishes performance in this experiment or if it is dependent on the shape of the airfoil. Whatever the reason for the low correlation value, it still seems unlikely that the results of the experiment are accurate as is, and further investigation would have to be made to determine if this was so.

Table 1. The lift to drag ratio, total flight time in seconds, speed in meters per second, and mass in grams are shown for each of the wing profiles.

Profile Name	Lift to Drag Ratio	Total Flight Time (s)	Speed (m/s)	Mass (g)
Profile 1A	0.102	646.96	6.58	145
Profile 1	0.256	615.38	6.54	133
Mod. Model 1	0.321	640.74	6.72	131
Mod. Model 2	0.010	648.36	6.77	128
Mod. Model 3	0.113	664.01	6.38	136
Mod. Model 4	0.313	677.09	6.90	128
Mod. Model 5	0.053	639.56	6.65	134

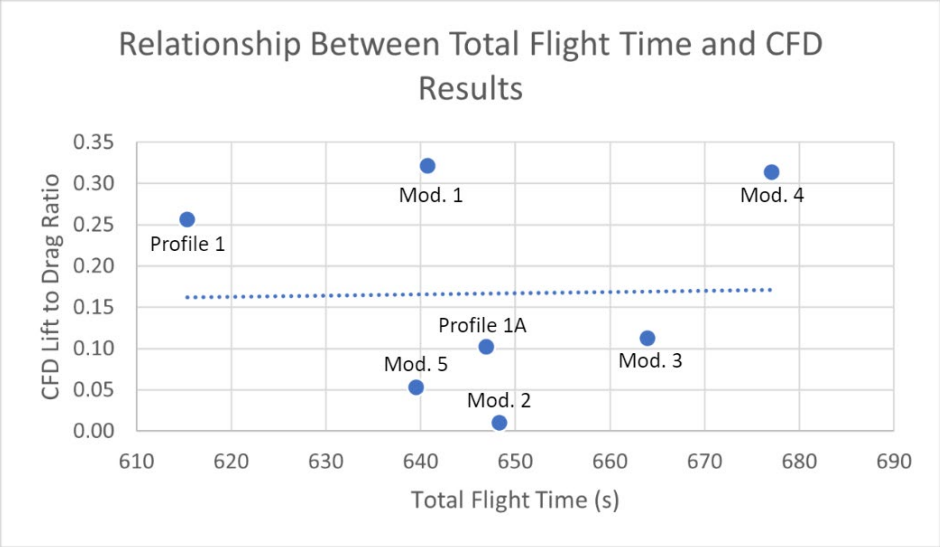

Figure 14. The line of best fit conveys the almost nonexistent correlation between the total flight times and lift to drag ratios.

Figure 15 expresses the association between the total flight time and the speed of each wing pair, indicating there was a minor connection among the variables in the MAV assessment. With a correlation coefficient of 0.30, there is a slight positive relationship where speed increases as flight time increases and vice versa, but not strong enough to make a well-informed assumption on what one variable is measured based on the other. However, when Mod. Model 3 was taken out of the equation, the correlation value became 0.86, suggesting that this wing pair was an outlier in the overall experiment. Therefore, the two variables may have a much stronger relationship than previously thought, one where there is a significant enough correlation to predict the other. Since total flight time and speed convey two measures of wing efficiency, it would only be natural for these values to have a stronger direct relationship, where more aerodynamically efficient wings would have higher values and less aerodynamically efficient wings would have lower values. A plausible explanation as to why Mod. Model 3 performed differently than the other wings is that the trials were conducted on the coldest of all the test days at around 44 degrees Fahrenheit, while the others were flown at 60 degrees Fahrenheit or higher. A lithium-ion battery may last longer in lower temperatures, but not enough data was collected to make this conclusion.

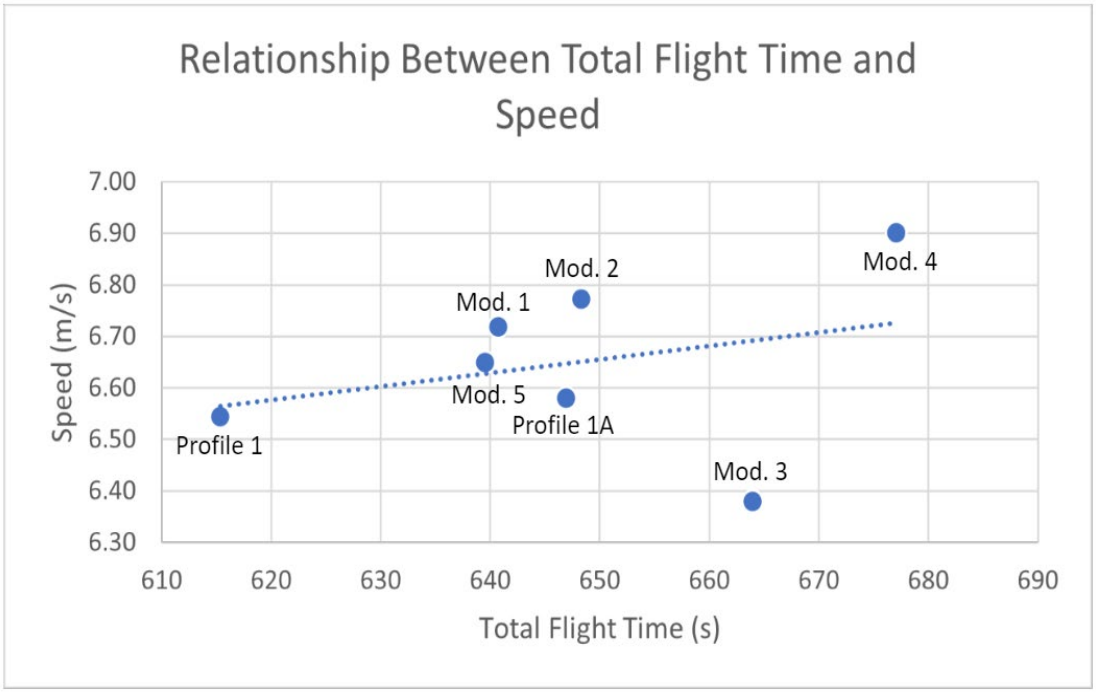

Figure 15. The line of best fit portrays a slight positive relationship between total flight time and speed.

The relationship between total flight time and mass was much smaller, with a correlation coefficient of –0.15, conveying a very weak indirect connection among the variables (see Figure 16). Thus, the low correlation value of the two variables reveals that one variable cannot accurately be predicted from the other. Since the range of the masses of each wing pair was relatively small, with only a 17-gram difference between the least to greatest wing pair mass, it was anticipated that there would be no significant correlation to total flight time. Simply put, there was not enough change in the mass between each wing pair to be able to determine how mass affects the total flight time.

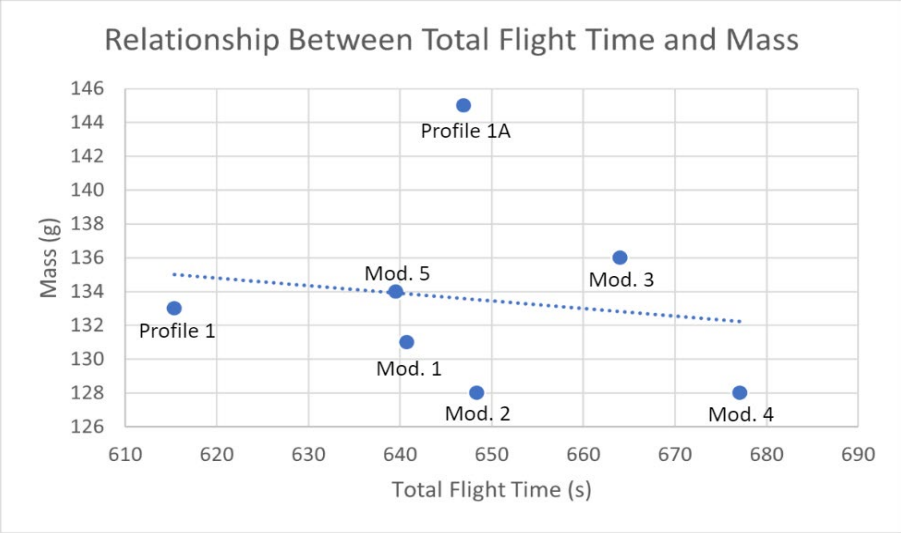

Figure 16. The line of best fit conveys an extremely weak negative relationship between total flight time and mass.

Figure 17 exhibits the connection between the speed and mass of each wing pair, demonstrating a much stronger link between the two than between the previous variables. With a correlation coefficient of –0.62, there is a moderately indirect relationship where the speed of a given wing pair decreases as the mass increases, and vice versa. This relationship is understandable as an increased amount of mass makes it more difficult to move at high speed, thus decreasing the rate at which the plane can fly. The correlation value is high enough that a general estimation could be made using one variable to get the other and be fairly accurate. This value becomes even stronger when the data for profile 1A is taken out of the analysis, as it is an outlier in the experiment. Without the wing pair, the correlation coefficient was calculated to be –0.92, a major change from the original value. This new value communicates that there is a very strong association between speed and mass, and that one variable would be able to be predicted from the other with high accuracy. Since profile 1A was the only smooth airfoil in the study, its aerodynamic properties are different from the corrugated airfoils and could explain why its behavior did not follow the trendline.

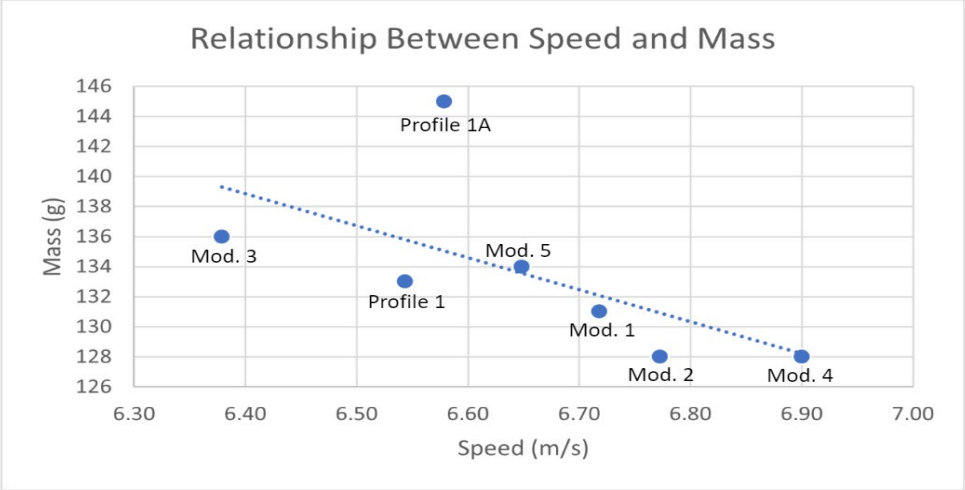

Figure 17. The line of best fit reveals a moderately strong relationship between the speed and mass of a profile.

Discussion

After experimentation, the present study can add valuable information to the available research on corrugated airfoils. The corrugated wings in this study were each characterized by a lower mass than the traditional wing, contradicting Rees' (1975b) statement that there is a slight increase in weight with these types of profiles. Therefore, benefits of corrugated profiles can be maximized by using less material, making the cost of production cheaper while also increasing aerodynamic efficiency, as demonstrated by the increased total flight time and decreased mass of Mod. Model's 2, 3, and 4 from profile 1A. Furthermore, the results of profile 1 support Okamoto et al.'s (1996) theory that a downward facing LE is more aerodynamically efficient than an upward facing LE. Profile 1 and Mod. Model 1 were the only profiles characterized by an upward facing LE, with profile 1 producing the shortest of the flights and Mod. Model 1 only performing better than profile 1 and Mod. Model 5 by 1.18 seconds.

The CFD analysis generated results consistent with those of Jain et al. (2015), who concluded that four of the five corrugated wings in their study were characterized by higher efficiency than the smooth airfoil. In

the present study, four of the corrugated profiles produced a higher lift to drag ratio and two corrugated profiles produced a lower lift to drag ratio than the smooth profile 1A. These findings suggest that the CFD results of corrugated profiles are more likely to have higher efficiencies than the CFD results of smooth airfoils. However, the overall lift to drag ratios of the present study were considerably lower than the lift to drag ratios of the wings in Kim et al.'s (2009) study, which was surprising as the profiles in the present study were based off this study's cross sections. The average lift to drag ratio of the present study was 0.167, while the average for the original study was 1.352, coming out to be an 87.65 percent decrease in average aerodynamic efficiency. Not only were the values lower, but they were also not consistent with Kim et al.'s (2009) findings. For example, Mod. Model 2 was found to have the highest lift to drag ratio in the original study but produced the lowest in the present study. Similarly, the original study recorded Mod. Model 1 as having the lowest lift to drag ratio, while the same profile generated the highest lift to drag ratio in the present study. Because the present study's CFD results did not align with Kim et al.'s (2009) results, it cannot be used to back up the conclusions from their study.

Although the CFD results were conflicting, they supported the conclusion of Kesel (2000) and Kim et al. (2009) that not all corrugations are equal in their aerodynamic efficiency. While some corrugated designs can increase performance, others diminish it, meaning certain designs are more beneficial than others, as shown by the fact there were corrugated profiles that performed better and worse than profile 1A. The study, however, was not able to determine specifically what characteristics of a corrugated airfoil cause this increased efficiency. In terms of addressing the gap in the research, the data was able to allude that the turbulent atmospheric layer does alter the aerodynamic efficiency of corrugated wings as Biradar et al. (2022) theorized. For instance, the CFD analysis measured Mod. Model 1 as having the greatest lift to drag ratio but flew for only the fifth longest total flight time. On the other hand, Mod. Model 2 had the lowest lift to drag ratio but ended up flying the third longest total flight time. CFD results, therefore, may not be an accurate means of determining efficiency in a real-world situation.

Conclusion

Limitations and Implications

There were a variety of setbacks when conducting this study, starting with creating the profiles within Autodesk Inventor. Neither Kesel (2000) nor Kim et al. (2009) provided dimensions of their wing cross sections, forcing this study's designs to be constructed with approximate measurements. It is not clear whether these minor differences significantly affected the results of the experiment or if they went unnoticeable. Once the airfoils seemed proportional to the original studies, the actual printing of the wings and plane body met another limitation. The 3D printer used was held by the researcher's high school engineering teacher and could only be run during school hours. As a result, a limited volume of material could be printed in a day, leading to the wing and plane having to be smaller than originally intended as a whole wing or part was required to be able to be printed in the allotted 8-hour school day. Smaller parts equated to a smaller wing surface area, decreasing lift and becoming a key reason as to why the plane could not take off and continue flying above the ground. Another issue with the 3D printing was that it was extremely difficult to separate the support filament from the printed part as it was not the type you could easily dissolve off but had to break it off in pieces. Thus, remnants of support filament remained attached to the wings during the MAV assessment, potentially increasing drag and affecting flight time and speed quantities.

With the testing period, the researcher's limited knowledge of electrical equipment and having no experience with flying a remote control plane led to a variety of issues. The preliminary tests consisted of multiple plane crashes that broke the plane, an electrical fire, and trouble with lifting off due to excessive weight of the combined parts. After a month of iterations, no significant progress was made, so the method had to be adjusted to where the plane was not required to take off and fly on its own, but still be within the turbulent

atmospheric layer to address the gap in the research. Another limitation with the experiment process was that there was only one battery used throughout the tests. The battery recharge wait time between trials made it difficult for multiple trials to be completed in a small time frame. Therefore, there were differing weather and temperature conditions amongst trials that could have affected results. It is also possible that the battery degraded with each use and may not have had an equal charge for each flight trial.

An implication of the study is that it ventured into the turbulent atmospheric layer, an area that none of the studies within the body of literature tested within. It suggests that CFD results may not be accurate when describing the efficiency of corrugated wings, and that they could have an even higher efficiency than believed to be when placed on an MAV design, such as the case with Mod. Models 2, 3, and 4. The study could open to more research on the potential benefits of corrugated wings on MAVs and lead to their implementation on these designs, increasing aerodynamic efficiency while simultaneously decreasing weight and cost.

Future Directions

Continuing the findings of this study by putting more of an emphasis on what makes a flyable remote control plane would further explore the effects of corrugated wings. By actually getting the plane off the ground and partaking in flight, a true picture of whether these types of wings increase efficiency can be made. Printing a larger plane by using a commercial 3D printer could make it easier to meet this goal by producing more lift from the increased surface area. Making the data more accurate through the use of multiple batteries and increasing the number of trials would provide a clearer picture of the relationship between CFD results and total flight time. Lastly, it would be interesting to see how conducting trials with the same pair of wings and differing temperatures would change total flight time results.

Acknowledgments

I would like to thank John Murnan for guiding me through the research process and making this project possible. I would also like to thank Donell Osborne and Rebecca Schwartz for reviewing my initial draft and offering suggestions that led to this final version.

References

Abd El-Latief, M. E., Elsayed, K., & Madbouli Abdelrahman, M. (2019). Aerodynamic study of the corrugated airfoil at ultra-low Reynolds number. *Advances in Mechanical Engineering, 11*(10), 1-18. https://doi.org/10.1177/1687814019884164

All3DP. (2022, July 5). *Best 3D printer filament: the main types in 2022*. https://all3dp.com/1/3d-printer-filament-types-3d-printing-3d-filament/

Benson, T. (Ed.). (2021, May 13). *The drag coefficient*. National Aeronautics and Space Administration. https://www.grc.nasa.gov/www/k-12/rocket/dragco.html

Biradar, G. S., Bankey, S., Mishra, A., Joshi, G., & Agrawal, A. (2022). Effect of free stream turbulence intensity on corrugated airfoils at ultra low Reynolds numbers. *Sādhanā*, *47*(2), 1-18. https://doi.org/10.1007/s12046-022-01861-y

Hall, N. (Ed.). (2022, October 20). *Lift coefficient*. Glenn Research Center. https://www1.grc.nasa.gov/beginners-guide-to-aeronautics/lift-coefficient/

Helmenstine, A. M. (2020, August 28). *What Is the Density of Air at STP?*. ThoughtCo. https://www.thoughtco.com/density-of-air-at-stp-607546

Jain, S., Bhatt, V., & Mittal, S. (2015). Shape optimization of corrugated airfoils. *Computational Mechanics*, *56*(6), 917–930. https://doi-org.proxygsu-sche.galileo.usg.edu/10.1007/s00466-015-1210-x

KendinYap. (2020, May 19). *How to make RC trainer airplane. DIY model airplane for beginners*. rcpano.net. https://www.rcpano.net/2020/05/19/how-to-make-rc-trainer-airplane-diy-model-airplane-for-beginners/

Kesel A. B. (2000). Aerodynamic characteristics of dragonfly wing sections compared with technical aerofoils. *The Journal of experimental biology*, *203*(20), 3125–3135. https://doi.org/10.1242/jeb.203.20.3125

Kim, W.-K., Ko, J. H., Park, H. C., & Byuan, D. (2009). Effects of corrugation of the dragonfly wing on gliding performance. *Journal of Theoretical Biology*, *260*(4), 523-530. https://doi.org/10.1016/j.jtbi.2009.07.015

Kurak, R. (2022, July 28). *Drag coefficient*. NASA Glenn Research Center. https://www1.grc.nasa.gov/beginners-guide-to-aeronautics/drag-coefficient/

Kurak, R. (2022, July 28). *Lift coefficient*. NASA Glenn Research Center. https://www1.grc.nasa.gov/beginners-guide-to-aeronautics/lift-coefficient/

Luo, G., & Sun, M. (2005). The effects of corrugation and wing planform on the aerodynamic force production of sweeping model insect wings. *Acta Mechanica Sinica*, *21*(6), 531–541. https://doi-org.proxygsu-sche.galileo.usg.edu/10.1007/s10409-005-0072-4

Okamoto, M., Yasuda, K., & Azuma, A. (1996). Aerodynamic characteristics of the wings and body of a dragonfly. *The Journal of experimental biology*, *199*(2), 281–294. https://doi.org/10.1242/jeb.199.2.281

Rees, C. J. C. (1975). Aerodynamic properties of an insect wing section and a smooth aerofoil compared. *Nature, 258*, 141–142. https://doi.org/10.1038/258141a0

Rees, C. J. C. (1975). Form and function in corrugated insect wings. *Nature, 256*, 200–203. https://doi.org/10.1038/256200a0

Rose, J. B. R., Natarajan, S. G., & Gopinathan, V. T. (2021). Biomimetic flow control techniques for aerospace applications: a comprehensive review. *Reviews in Environmental Science& Biotechnology*, *20*(3), 645–677. https://doi-org.proxygsu-sche.galileo.usg.edu/10.1007/s11157-021-09583-z